Dyes and Pigments 82 (2009) 316–321

Contents lists available at ScienceDirect

Dyes and Pigments

journal homepage: www.elsevier.com/locate/dyepig

The facile synthesis and high efficiency of the red electroluminescent dopant DCINB: A promising alternative to DCJTB

Ping Zhao [a], Hao Tang [b], Qiong Zhang [a], Yajuan Pi [a], Min Xu [a], Runguang Sun [b], Weihong Zhu [a,*]

[a] Key Laboratory for Advanced Materials and Institute of Fine Chemicals, East China University of Science & Technology, Shanghai 200237, PR China
[b] School of Materials Science and Engineering, Shanghai University, Shanghai 201800, PR China

ARTICLE INFO

Article history:
Received 13 December 2008
Received in revised form
21 January 2009
Accepted 27 January 2009
Available online 11 February 2009

Keywords:
Synthesis
Indoline
Dopant
Red emitter
Electroluminescence
Optical properties

ABSTRACT

The cost of manufacturing 4-(dicyanomethylene)-2-*tert*-butyl-6-(1,1,7,7-tetramethyljulolidyl-9-enyl)-4*H*-pyran (DCJTB) is prohibitively high because the synthesis of one of the key intermediates, 1,1,7,7-tetramethyljulolidine, is costly, produces by-products and is of low yield. As an alternative low-cost process, a novel red dopant 4-(dicyanomethylene)-2-*tert*-butyl-6-(8-(4-methyl)phenyl-2,3-dihydro-1*H*-cyclopenta [3*a*,8*a*]indolin-5-enyl)-4*H*-pyran (DCINB) bearing an indoline unit instead of 1,1,7,7-tetramethyljulolidine as electron donor has been conveniently synthesized in high yield. The dopant exhibited very similar absorption and emission behaviour to DCJTB, but displayed superior fluorescence quantum yield and electroluminescence efficiency, which was attributed to high recombination ratio of excitons imparted by the introduced indoline unit. The synthesis and purification stages are simple and can be scaled-up, thereby offering a possible alternative to the commercial DCJTB.

1. Introduction

Organic light-emitting devices (OLEDs) have attracted considerable attention because of their potential applications in flat-panel displays. During the past decade, the study on high efficient organic electroluminescent (EL) materials has become one of the foremost topics in chemistry and physics [1–4], and much progress has been made [5,6]. For full color displays, it is necessary to have a set of primary green, blue and red emitters with sufficiently high luminous efficiency and proper chromaticity. At present, organic materials for green and blue OLEDs with high efficiency, saturated emission and practical lifetime have been developed rapidly [7,8]. However, the development of organic materials for red electroluminescence is far behind in terms of both color purity and efficiency, and the performance of red OLEDs is still not satisfactory [9]. Most of red fluorophores with narrow band gap are highly susceptible to concentration quenching, and become either weak or even not emissive at all in solid state [9,10]. In order to prevent the concentration quenching, doping a red emitter with strong fluorescence into a suitable host as the emitting layer is a common method to obtain high-performance red OLEDs [10–12]. There has been intensive study in developing organic red dopants, such as pyran-containing compounds [13–16], europium chelate complexes [17–19], and porphyrin compounds [20–22]. The pyran-containing compounds, such as 4-(dicyanomethylene)-2-methyl-6-(4-(dimethylaminostyryl)-4*H*-pyran) (DCM) analogues, typically consisting of two parts of an electron donor unit and an electron acceptor unit, are regarded as one of the most important red dopants for OLED applications. Up to date, 4-(dicyanomethylene)-2-*tert*-butyl-6-(1,1,7,7-tetramethyljulolidyl-9-enyl)-4*H*-pyran (DCJTB) with solution PL $\lambda_{max} \sim 630$ nm and a quantum efficiency >90% is still one of the most efficient red dopants of tris(8-hydroxyquinolinato) aluminum (Alq3) hosted OLEDs [10,23,24]. However, the cost of manufacturing DCJTB is prohibitively high owing to the synthetic complication of one of the key intermediates, 1,1,7,7-tetramethyljulolidine (TMJ), which is tedious to synthesize with too many by-products and a low yield [25–27]. Accordingly, it is very desirable to develop high efficient red alternative to DCJTB with convenient and low-cost synthetic processes. Presently, many structural modifications have been attempted on their electron-accepting or electron-donating groups of dicyanomethylene-pyran derivatives. For example, Lee et al. reported a family of red dopants with a longer conjugation moiety benzopyran (4-dicyanomethylene-chromene) as electron acceptor to explore a better red chromaticity (longer wavelength) than

* Corresponding author. Tel.: +86 21 64250772; fax: +86 21 64252758.
E-mail address: whzhu@ecust.edu.cn (W. Zhu).

0143-7208/$ – see front matter © 2009 Elsevier Ltd. All rights reserved.
doi:10.1016/j.dyepig.2009.01.016

(4-(dicyanomethylene)-2-methyl-6-(2-(2,3,6,7-tetrahydro-1*H*,5*H*-benzo[ij]quinolizin-9-yl)ethenyl)-4*H*-pyran) (DCM2) and DCJTB [14]. Huang et al. introduced a (diethylamino)-2-alkoxy segment as electron donor in the red dopant materials with the advantages of high yield, convenient synthesis and narrow FWHM [16]. However, EL performances and efficiencies are still not yet comparable to DCJTB.

Herein we reported the facile synthesis and high EL performance of a red EL emitter, 4-(dicyanomethylene)-2-*tert*-butyl-6-(8-(4-methyl)phenyl-2,3-dihydro-1*H*-cyclopenta[3*a*,8*a*]indolin-5-enyl)-4*H*-pyran (DCINB; Fig. 1). The 4-(dicyanomethylene)-2-*tert*-butyl-6-methyl-4*H*-pyran unit in DCJTB was retained as electron acceptor and an indoline unit instead of introducing TMJ as electron donor. With respect to the traditional red dopant DCJTB, the synthesis and purification of DCINB were simple and amenable to scale-up. Specifically, the luminance and the current efficiency of an EL device fabricated with DCINB were 1.8 and 4.6 times, respectively, greater than that of DCJTB with almost the same EL peak, indicative of a promising alternative to DCJTB.

2. Experimental

2.1. General procedure

Both 4-(dicyanomethylene)-2-*tert*-butyl-6-methyl-4*H*-pyran (**3**) and 8-(4-methyl)phenyl-2,3-dihydro-1*H*-cyclopenta[3*a*,8*a*]indoline (**1**) were prepared as reported in the literature [28–30]. All reagents and solvents were analytical grade chemicals. ^{1}H NMR and ^{13}C NMR measurements were recorded on a Bruker AV-400 spectrometer in $CDCl_3$ with tetramethylsilane (TMS) as internal standard. Mass spectra measurements were carried out on Micromass LCT. UV–vis absorption and fluorescence spectra were measured using a Varian Cary 100 UV–vis spectrophotometer and Varian Cary Eclipse fluorescence spectrophotometer, respectively. Cyclic voltammograms were recorded with VersaStat II at a constant scan rate of 100 mV/s. Measurements were performed in a conventional three-electrode cell. The working electrode was platinum electrode coated with a thin film of DCINB; the counter electrode was platinum wire and the reference electrode was Ag/AgCl with a solution containing 0.1 M (n-Bu)$_4$NPF$_6$ in acetonitrile as the supporting electrolyte.

2.2. 5-Formyl-8-(4-methyl)phenyl-2,3-dihydro-1H-cyclopenta[3a,8a]indoline (2)

Phosphorus oxychloride (ed note; reacts violently with water; incompatible with many metals, alcohols, amines, bases and solvents; toxis; corrosive; 20 mL, 200 mmol) was added to *N*,*N*-dimethylformamide (35 mL, 443 mmol) at 0 °C, and the ensuing solution was stirred at room temperature for 15 min. A solution of 8-(4-methyl)phenyl-2,3-dihydro-1*H*-cyclopenta[3*a*,8*a*] indoline (11.6 g, 46.5 mmol) in dichloromethane (120 mL) was added to the reaction solution. After stirring at 95 °C for 5 h, the solution was poured into ice water, neutralized with aqueous NaOH (10 wt%) and then the mixture was extracted with dichloromethane. The organic layer was washed with water and brine, successively, and dried over anhydrous $MgSO_4$. After removing solvents, the resulting intermediate **2** was obtained from recrystallization with ethanol. Yield: 78% (10.0 g). ^{1}H NMR (400 MHz, $CDCl_3$, ppm): δ 9.69 (s, 1H, –CHO), 7.63 (s, 1H), 7.51 (d, $J = 8.4$ Hz, 1H), 7.16–7.23 (m, 4H), 6.73 (d, $J = 8.8$ Hz, 1H), 4.91 (t × d, $J = 8.4$, 1.6 Hz, 1H), 3.84 (t × d, $J = 7.8$, 1.6 Hz, 1H), 2.37 (s, 3H), 1.49–2.12 (m, 6H).

2.3. DCINB

A mixture of **2** (1.0 g, 3.6 mmol), **3** (0.77 g, 3.6 mmol), piperidine (2 mL), acetic acid (1 mL) and toluene (40 mL) was refluxed under argon for 5 h. Then the reaction mixture was cooled to room temperature, and the solid was filtered. Solid DCINB was obtained after recrystallization with toluene. Yield: 86% (1.44 g). m.p. 255–257 °C. ^{1}H NMR (400 MHz, $CDCl_3$, ppm) δ: 7.36–7.32 (d, $J = 16.0$ Hz, 1H, –CH═), 7.33 (s, 1H, phenyl-H), 7.21–7.19 (dd, $J = 8.4$, 1.6 Hz, 1H, phenyl-H), 7.20–7.17 (m, 4H, phenyl-H), 6.79 (d, $J = 8.4$ Hz, 1H, phenyl-H), 6.60 (d, $J = 2.0$ Hz, 1H, pyran-H), 6.52 (d, $J = 2.0$ Hz, 1H, pyran-H), 6.51 (d, $J = 6.0$ Hz, 1H, –CH═), 4.87–4.90 (m, 1H, –CH–), 3.82–3.86 (m, 1H, –CH–), 2.36 (s, 3H, –CH_3), 1.68–2.09 (m, 6H, –CH_2–), 1.38 (s, 9H, –C(CH_3)$_3$). ^{13}C NMR (100 MHz, $CDCl_3$, ppm) δ: 171.79, 160.33, 156.74, 150.92, 138.96, 138.54, 136.03, 133.19, 129.99, 124.65, 123.70, 121.46, 115.78, 115.76, 112.51, 106.95, 105.34, 102.34, 69.70, 57.64, 44.96, 36.62, 35.30, 33.36, 28.13, 24.31, 20.89. IR (KBr pellet): 3025.4, 2975.6, 2934.1, 2855.3, 2195.8 (–C≡N), 2187.6 (–C≡N), 1638.2, 1596.4, 1552.4, 1513.3, 1491.6, 1383.8, 1327.4, 1195.7, 1125.7, 1101.4, 966.1, 928.5, 852.8, 838.6,

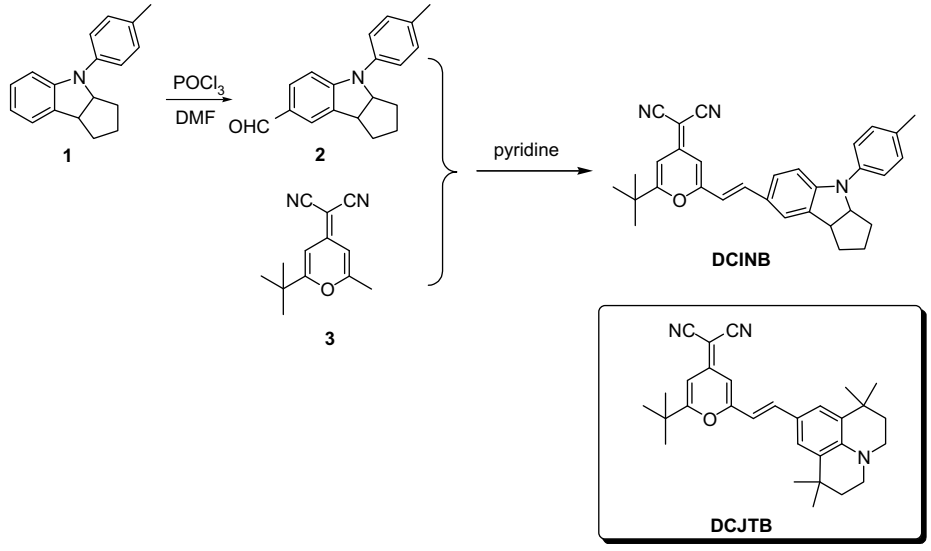

Fig. 1. Synthetic route of red dopant DCINB and the chemical structure of DCJTB as reference.

802.4 cm^{-1}. ESI HRMS Calcd for $C_{32}H_{31}N_3O$ $[M+H]^+$: 474.2545; Found: 474.2541.

2.4. OLEDs fabrication and measurement

Alq3 and fluorescent materials DCJTB were commercially purchased from Kodak, and purified by train sublimation. The devices were fabricated on indium tin oxide (ITO) coated glass substrate with a sheet resistance of ~80 Ω/□. The substrates were cleaned via ultrasonic with super-purity water. All organic layers were evaporated onto the substrates by conventional resistive heating in the same vacuum chamber (1×10^{-3} Pa), and then, Al cathode was deposited without breaking the vacuum. The evaporating speed and thickness of the organic and metal layers were monitored by quartz oscillators. The EL configuration structure of the device was ITO (100 nm)/NPB (40 nm)/Alq3: dopant (30 nm)/Alq3 (30 nm)/LiF (1 nm)/Al(100 nm), in which the NPB and Alq3 were separately used as the hole-transporting layer and the electron-transporting layer, respectively. EL emission spectra with Commission Internationale de l'Eclairage (CIE) coordination and luminance–voltage characteristics of the devices without encapsulation were measured with JY SPEX CCD3000 spectrometer and ARRAY 3645A source meter and FLUKE 45 multimeter. Effective emissive area was 5×5 mm^2, and all measurements were carried out in ambient atmosphere at room temperature after vacuum break.

3. Results and discussion

3.1. Synthesis

The synthetic route of the titled compound DCINB and the reference structure of DCJTB are shown in Fig. 1. The dicyanomethylene-pyran derivatives (DCM analogues) have the typical donor–π-acceptor (D–π-A) structure, resulting in their typical emission band ascribed to the intramolecular charge transfer (ICT). Generally, the emission wavelength of these analogues can be tuned by changing either the donor moiety or the acceptor moiety. In DCJTB, 4-(dicyanomethylene)-2-*tert*-butyl-6-methyl-4*H*-pyran unit is a good acceptor moiety containing a sterically hindered *tert*-butyl substituent. The steric hindrance can be further enhanced with the assistance of the tetramethyl and two six-membered locking rings from julolidine unit. However, the synthesis of 1,1,7,7-tetramethyljulolidine (TMJ) is tedious with too many by-products and a low yield [25–27]. For the sake of meeting convenient scale-up and low-cost synthetic processes, it is very necessary to develop high efficient red alternative to DCJTB. As illustrated in Fig. 1, we maintained the acceptor and replaced TMJ with an indoline unit as the electron donor part. The key indoline intermediate of 5-formyl-8-(4-methyl)phenyl-2,3-dihydro-1*H*-cyclopenta[3*a*,8*a*]indoline (**2**) was conveniently prepared via Vilsmeier reaction from the precursor **1** as reported in the literature [29,30]. Actually, in our pilot plant, we have successfully scaled the preparation of the intermediate **2** up to hundreds of kilograms. The target

Table 1
Data of steady-state absorption, fluorescence, luminescent efficiency in 1,2-dichloroethane (5×10^{-6} mol/L) and energy levels of DCINB and DCJTB.

Emitters	λ_{max}^{abs}/nm (log ε)	λ_{max}^{em}/nm	η[a] (%)	HOMO (eV)	LUMO (eV)
DCINB	500 (4.57)	622	1.08	−5.16[b]	−3.10[c]
DCJTB	509 (4.54)	622	1.0	−5.11	−3.10[c]

[a] The relative luminescent efficiency (η) was obtained by comparing with DCJTB.
[b] Derived from the onset oxidation voltages using Ag/AgCl as reference electrode.
[c] Derived from the transition energy of the lowest absorption band.

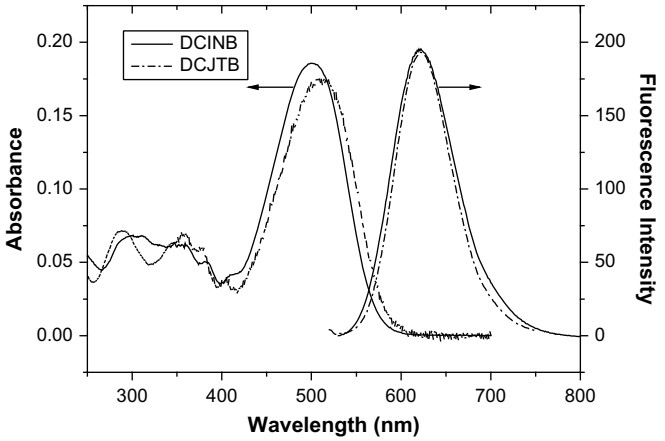

Fig. 2. UV–vis absorption and luminescence spectra of DCINB and DCJTB in 1,2-dichloroethane (5×10^{-6} mol/L).

emitter of DCINB was finally obtained via the traditional Knoevenagel reaction [31] with a high yield of 86%. Its chemical structure was fully characterized by ^1H NMR, ^{13}C NMR, IR, and HRMS (shown in Experimental section). The characteristic coupling constant ($J = 16.0$ Hz) in the ^1H NMR spectrum of DCINB is indicative of the predominant *trans*-isomer. It is worthy of mention that the synthesis of this novel material DCINB is quite straightforward and capable of scale-up since it can be simply purified via the common recrystallization method, which makes DCINB quite attractive as a practical and promising alternative to DCJTB for red EL dopants.

3.2. Photophysical characteristics and energy levels

The optical properties of DCINB were examined by steady-state absorption and luminescence spectra in dilute 1,2-dichloroethane. For comparison, DCJTB was measured under the same condition, and the related photophysical data are summarized in Table 1. The fluorescent efficiency of DCINB was obtained with DCJTB as

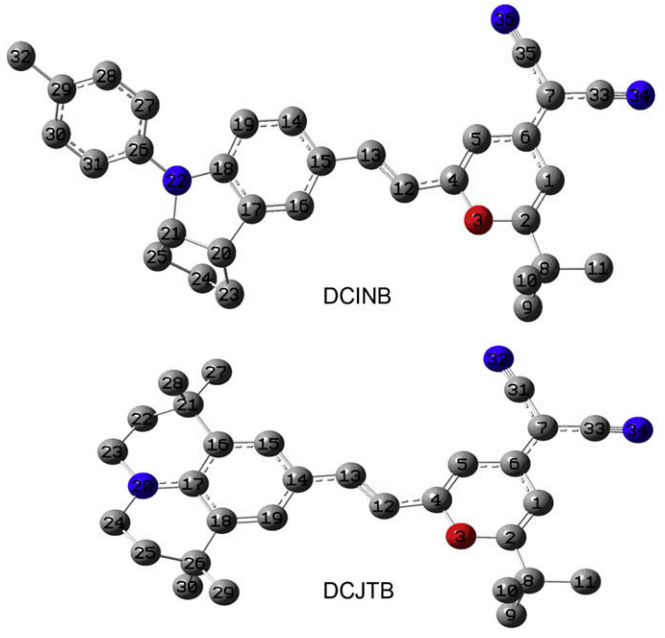

Fig. 3. Optimized ground-state geometries of DCINB and DCJTB obtained with B3LYP/6-31G (d), hydrogens are omitted for clarity.

Table 2
Important dihedral angles in the optimized ground-state geometries of DCINB and DCJTB.

DCINB		DCJTB	
C26–N22–C18–C19	−22.89°	C23–N20–C17–C16	10.23°
C21–N22–C18–C17	−9.38°	C24–N20–C17–C18	9.72°
C14–C15–C13–C12	178.32°	C15–C14–C13–C12	179.22°
C13–C12–C4–C5	−3.55°	C13–C12–C4–C5	−2.49°
C13–C12–C4–O3	176.62°	C13–C12–C4–O3	177.75°
C5–C6–C7–C35	0.15°	C5–C6–C7–C31	0.14°
C1–C6–C7–C33	−0.01°	C1–C6–C7–C33	0.01°

a standard. As a DCM analogue, DCINB shows a typical absorption band at 500 nm (Fig. 2), blue-shifted by 9 nm with respect to DCJTB, resulting from the ICT transition of the D–π-A structure. However, the molar extinction coefficients (Table 1) and emission spectra of DCINB and DCJTB in dilute 1,2-dichloroethane are almost identical with the same peak at 622 nm. Specifically, the relative luminescent efficiency of DCINB is 8% higher than that of DCJTB (Table 1).

Cyclic voltammograms (CV) is used to investigate the redox behaviour of the new emitter DCINB and to assess the highest occupied molecular orbital (HOMO) energy level. The oxidation onset potential determined in acetonitrile by CV is 0.76 V, and the corresponding HOMO energy level *vs.* vacuum level is −5.16 eV calculated from the measured onset potential of oxidation according to an empirical formula, HOMO = −e(E_{ox} + 4.4) eV [32]. The corresponding lowest unoccupied molecular orbital (LUMO) energy level of DCINB is −3.10 eV calculated using the HOMO energy level along with the energy gap (E_g) derived from the edge of absorption spectra. Exactly, the HOMO and LUMO energy levels of DCINB and DCJTB are essentially same (Table 1), indicating that the change of TMJ unit with an indoline unit as the electron donor part doesn't have heavy effect on the orbital energy level.

3.3. Theoretical calculations

In an attempt to understand the geometrical, electronic, and optical properties of DCINB and DCJTB at a molecular level, we performed DFT calculations on the two chromophores and time-dependent DFT (TDDFT) calculations of their excited states, using the Gaussian 03 program package [33]. Hybrid B3LYP exchange-correlation functional [34] and a 6-31G (d) basis set [35] were employed in consideration of both accuracy and efficiency.

Fig. 3 shows the optimized ground-state geometries of DCINB and DCJTB while the main characteristic dihedral angles are tabulated in Table 2. As indicated by the dihedral angles, these two molecules are in general plane, forming large conjugation systems, which lend themselves to efficient intramolecular electron transfer. Exceptionally the dihedral angle of C26–N22–C18–C19 (−22.89°) in DCINB is large. The major distinction caused by the replacement of TMJ with indoline unit is that the donor part in DCINB is tilted out of the main plane, especially, the benzene ring and the five-membered ring in the indoline unit. This structural feature is beneficial to the suppression of the concentration quenching.

The topologies of the calculated frontier orbitals are sketched in Fig. 4. In both molecules, the HOMOs are mainly localized within the electron-donating fraction, while the LUMOs are mainly localized within the electron-withdrawing fraction. It is clear that in DCINB the conjugation has been further extended by the phenyl ring substitution on the nitrogen of the donor moiety. For both molecules, the HOMO energies are reasonably well predicted by theoretical approaches. Nevertheless, LUMO energies are underestimated by calculation. The TDDFT absorption spectra show that the λ_{max} transition corresponds to a HOMO → LUMO single excitation for both molecules, indicating the great extent of intramolecular charge transfer upon excitation. The calculated λ_{max} for DCJTB (509 nm) is in very good agreement with the experimental data (509 nm). However, the calculated lowest transition for DCINB is red-shifted by about 35 nm compared to the measured value. This is in accordance with the more extended charge-transfer character of this transition in DCINB, which is not properly captured by TDDFT calculations employing current exchange-correlation functional [36].

According to Marcus theory, the hole and electron transporting velocity is determined by

$$K = \left(\frac{\pi}{\lambda K_b T}\right)^{1/2} \frac{V^2}{h} \exp\left(-\frac{\lambda}{4K_b T}\right)$$

where λ, K_b, V and T denote the reorganization energy, Boltzmann constant, coupling constant and temperature, respectively. As

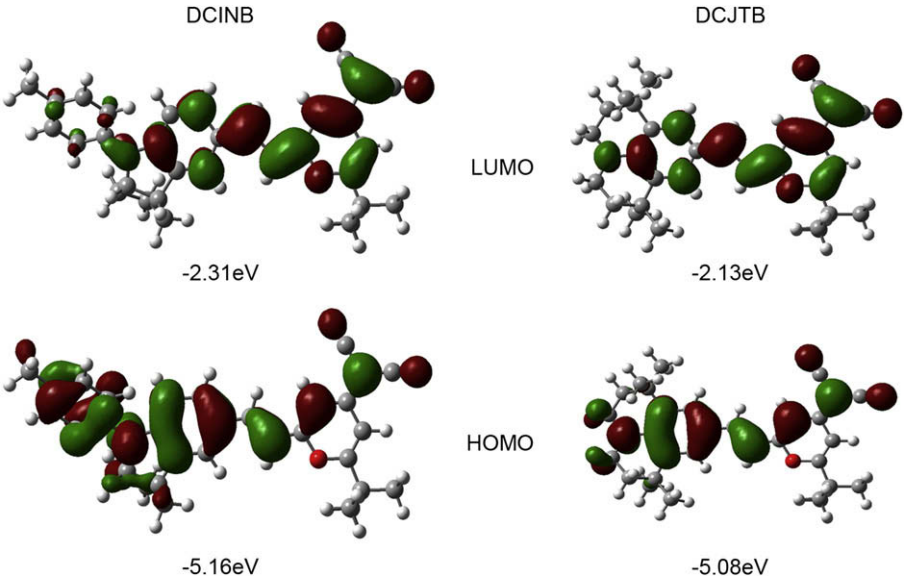

Fig. 4. Isodensity surface plots and energy of HOMO and LUMO orbitals of DCINB and DCJTB (isodensity = 0.025 a.u.).

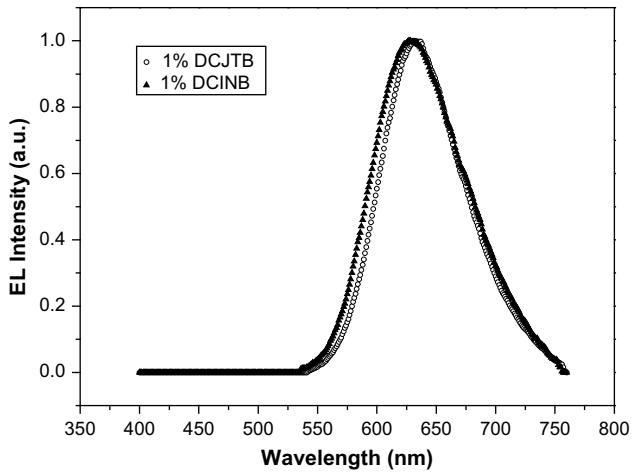

Fig. 5. EL spectra based on DCINB and DCJTB with 1 wt% doping concentration.

indicated by this formula, the smaller the reorganization energy is, the faster the transporting velocity of the charge carriers will be. The reorganization energies of DCINB, λ_{hole} and $\lambda_{electron}$, are calculated to be 107 and 401 meV, respectively, which are both smaller than those of DCJTB (177, 421 meV, respectively). Therefore, our calculation demonstrated that DCINB will have better charge carrier transporting property than DCJTB.

3.4. *EL performances of DCINB* vs. *DCJTB*

For comparison, the multi-layer organic EL devices were fabricated by vapor deposition with a configuration of ITO/NPB (40 nm)/Alq3:1 wt% DCINB or DCJTB (30 nm)/Alq3 (40 nm)/LiF (1 nm)/Al (100 nm). *N*,*N*′-Bis(1-naphthyl)-*N*,*N*′-diphenyl-1,1′-biphenyl-4,4′-diamine (NPB) served as a hole transporter, and Alq3 as host matrix and electron transporter. Interestingly, the EL spectral sketch based on DCINB and DCJTB with doping concentrations of 1 wt% is superimposed with peak at 629 and 631 nm, respectively (Fig. 5). The maximum EL emissions of the devices are about 630 nm, with the corresponding Commission Internationale de l'Eclairage (CIE 1931) coordinates of (0.61, 0.38) and (0.62, 0.37), respectively, which fell into the red region. It seems that there is no trace of Alq3 emission at 520 nm because of complete energy transfer from the Alq3 host to the dopants, thus leading to the improvement of color purity.

Fig. 6 shows their relative luminance–voltage characteristics. The maximum luminance of EL devices based on the new emitter DCINB can reach 6276 cd/m^2 at the driving voltages of 14 V, which was about 1.8 times as that of DCJTB. However, the onset voltage of EL device fabricated with DCINB is about 4.9 V, which is higher than that with DCJTB (~3.5 V). As known for the dopant emitter in the host of Alq3, there are two channels resulting in luminescence: 1) Injected electrons and holes combine on the host molecules Alq3. The excitons are formed on Alq3 sites and then excitonic energy is transferred to the dopant sites by the Föster energy transfer process and the dopant molecules produce the red light. 2) Injected carriers directly combine on the dopant molecules and then form excitons followed by red light emission from the dopant molecules, which always brings high driving voltage [37,38]. It is understood that the incorporated indoline unit in DCINB might increase the latter channel, that is, direct recombination ratios and capability of carriers under high driving voltage, resulting in better performance in luminescence than that of the Kodak's traditional red dopant of DCJTB.

Moreover, the current efficiency for DCINB was increased sharply comparing with that of DCJTB (Fig. 7). The highest current efficiency based on DCINB can reach 3.53 cd/A at low current density, almost 4.6 times as that of DCJTB (0.76 cd/A). Although the current efficiency for DCINB became decreased when increasing current density, the current efficiency based on DCINB at 240 mA/cm^2 was still remained at 2.35 cd/A (Fig. 7). Obviously, EL devices based on DCINB have achieved much better performance in both luminance and current efficiency. As mentioned above, the luminescence and efficiency of EL devices in the host–dopant system are dependent on the energy transfer between the host and dopants, and the injection amounts and balance of carriers. Here, the better EL performances for DCINB can be attributed to the introduced electron donor of indoline unit, resulting in the high recombination ratio of excitons.

Like DCJTB, EL devices based on the dopant of DCINB exhibit a nearly flat response of current efficiency with respect to a wide range of driving current density from 10 mA/cm^2 (an earlier plateau) to 300 mA/cm^2, which might be highly beneficial to the application of passive matrix devices requiring high excitation density [15]. Also, EL performance may be further improved by choosing appropriate host material, hole injection material, cathodes as well as device optimization.

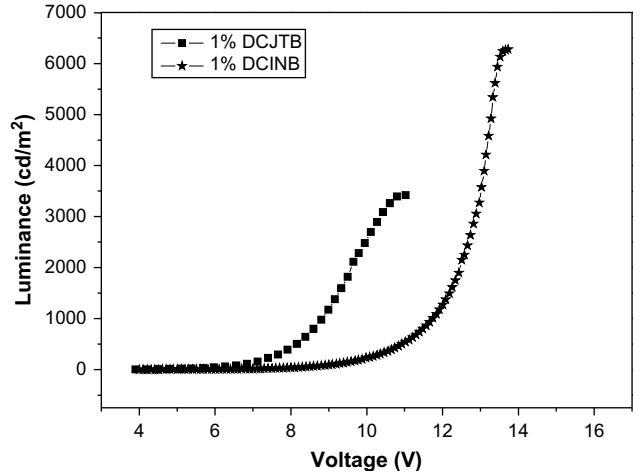

Fig. 6. Luminance–voltage of EL devices based on DCINB and DCJTB with 1 wt% doping concentration.

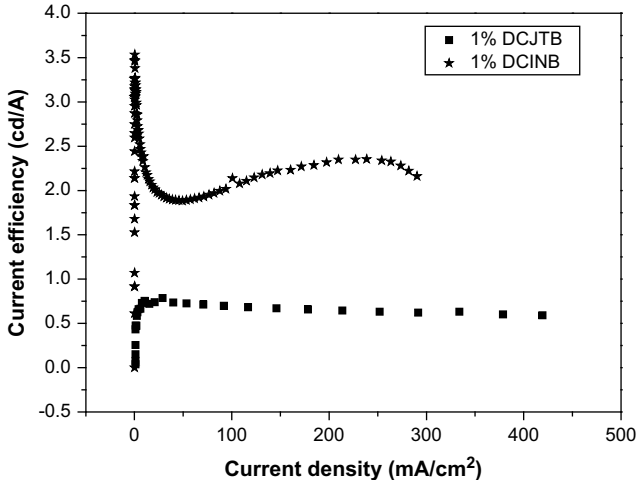

Fig. 7. Current efficiency–current density characteristics of EL devices based on DCINB and DCJTB with 1 wt% doping concentration.

4. Conclusions

A novel red dopant DCINB was synthesized by introducing an indoline moiety as electron donor and 4-(dicyanomethylene)-2-*tert*-butyl-6-methyl-4*H*-pyran as its electron acceptor. DCINB exhibits very similar absorption and emission behaviour to DCJTB, but has higher fluorescence quantum yield and superior EL luminance and efficiency. Like DCJTB, EL devices based on the dopant of DCINB exhibit a nearly flat response of current efficiency with respect to a wide range of driving current density from 10 mA/cm^2 (an earlier plateau) to 300 mA/cm^2, which might be highly beneficial to the high excitation density for passive matrix devices. Notably, the luminance and the current efficiency of EL devices fabricated with red dopant emitter DCINB are 1.8 and 4.6 times as that of DCJTB, respectively. It was also proved that the synthesis and purification procedures of DCINB were very simple with high yield, and capable of scale-up.

Acknowledgements

We thank the support from NSFC/China, the Program for New Century Excellent Talents in University (NCET-06-0418), Shanghai Shuguang Project (07SG34), and Specialized Research Fund for the Doctoral Program of Higher Education (SRFDP 200802510011).

References

[1] VanSlyke SA, Chen CH, Tang CW. Organic electroluminescent devices with improved stability. Appl Phys Lett 1996;69:2160–2.
[2] Young RH, Tang CW, Marchetti AP. Current-induced fluorescence quenching in organic light-emitting diodes. Appl Phys Lett 2002;80:874–6.
[3] Kwon TW, Alam MM, Jenekhe SA. n-Type conjugated dendrimers: convergent synthesis, photophysics, electroluminescence, and use as electron-transport materials for light-emitting diodes. Chem Mater 2004;16:4657–66.
[4] Tao YT, Wang Q, Yang CL, Zhang K, Wang Q, Zou TT, et al. Solution-processable highly efficient yellow- and red-emitting phosphorescent organic light emitting devices from a small molecule bipolar host and iridium complexes. J Mater Chem 2008;18:4091–6.
[5] Meng H, Herron N. Organic small molecule materials for organic light-emitting diodes. Opt Sci Eng 2007;111:295–412.
[6] D'Andrade B. White phosphorescent LEDs offer efficient answer. Nat Photonics 2007;1:33–4.
[7] Su YJ, Huang HL, Li CL, Chien CH, Tao YT, Chou PT, et al. Highly efficient red electrophosphorescent devices based on iridium isoquinoline complexes: remarkable external quantum efficiency over a wide range of current. Adv Mater 2003;15:884–8.
[8] Wen SW, Lee MT, Chen CH. Recent development of blue fluorescent OLED materials and devices. J Disp Technol 2005;1:90–9.
[9] Park JH, Seo JH, Lim SH, Ryu GY, Shin DM, Kim K. The effect of the molecular structure of organic material on the properties of solid-state fluorescence and electroluminescence. J Phys Chem Solids 2008;69:1314–9.
[10] Chen CT. Evolution of red organic light-emitting diodes: materials and devices. Chem Mater 2004;16:4389–400.
[11] Lee YG, Kang SK, Oh TS, Lee HN, Lee S, Koh KH. Comparison of two cohost systems for doped red organic light-emitting devices in an effort to improve the efficiency and the lifetime. Org Electron 2008;9:339–46.
[12] Zhao YX, Peng P, Zhou YH, Wu WC, Tian WJ. Energy transfer and luminescent properties in PVK and novel donor–acceptor molecular materials blend system. Chem J Chin Univ 2007;28:1345–9.
[13] Wang BC, Liao HR, Chen WH, Chou YM, Yeh JT, Chang JC. Theoretical investigation of electro-luminescent properties in red emission DCM, DCJ, RED and DAD derivatives. J Mol Struct Theochem 2005;716:19–25.
[14] Zhang XH, Chen BJ, Lin XQ, Wong OY, Lee CS, Kwong HL, et al. A new family of red dopants based on chromene-containing compounds for organic electroluminescent devices. Chem Mater 2001;13:1565–9.
[15] Li JY, Liu D, Hong ZR, Tong SW, Wang PF, Ma CW, et al. A new family of isophorone-based dopants for red organic electroluminescent devices. Chem Mater 2003;15:1486–90.
[16] Yang L, Guan M, Nie D, Lou B, Liu Z, Bian Z, et al. Efficient, saturated red electroluminescent devices with modified pyran-containing emitters. Opt Mater 2007;29:1672–9.
[17] Xin H, Li FY, Shi M, Bian ZQ, Huang CH. Efficient, saturated red electroluminescent devices with modified pyran-containing emitters. J Am Chem Soc 2003;125:7166–7.
[18] Kido J, Okamoto Y. Organo lanthanide metal complexes for electroluminescent materials. Chem Rev 2002;102:2357–68.
[19] Li SF, Zhong GY, Zhu WH, Li FY, Pan JF, Huang W, et al. White light electroluminescence from a dendritic europimn complex. Chem Lett 2005;34:688–9.
[20] O'Brien DF, Baldo MA, Thompson ME, Forrest SR. Improved energy transfer in electrophosphorescent devices. Appl Phys Lett 1999;74:442–4.
[21] Baldo MA, O'Brien DF, You Y, Shoustikov A, Sibley S, Thompson ME, et al. Highly efficient phosphorescent emission from organic electroluminescent devices. Nature 1998;395:151–4.
[22] Kim DU, Paik SH, Kim SH, Tak YH, Kim SD, Han YS, et al. Electroluminescent characteristics of novel platinum–porphyrin complex. Colloids Surf A 2008; 313:444–7.
[23] Yao YS, Zhou QX, Wang XS, Wang Y, Zhang BW. A DCM-type red-fluorescent dopant for high-performance organic electroluminescent devices. Adv Funct Mater 2007;17:93–100.
[24] Liu TH, Iou CY, Chen CH. Doped red organic electroluminescent devices based on a cohost emitter system. Appl Phys Lett 2003;83:5241–3.
[25] Chen CH, Tang CW, Shi J, Klubek KP. Recent developments in the synthesis of red dopants for Alq(3) hosted electroluminescence. Thin Solid Films 2000;363:327–31.
[26] Balaganesan B, Wen SW, Chen CH. Synthetic study of tetramethyljulolidine-a key intermediate toward the synthesis of the red dopant DCJTB for OLED applications. Tetrahedron Lett 2003;44:145–7.
[27] Chen CH, Klubek KP, Shi JM. Red organic electroluminescent materials. U.S. Patent. No. 5908581; 1999.
[28] Miles ML, Harris TM, Hauser CR. Aroylations at the methyl group of benzoylacetone and related β-Diketones with esters to form 1,3,5-triketones by sodium hydride. Other terminal condensations. J Org Chem 1965;30:1007–11.
[29] Horiuchi T, Miura H, Uchida S. Highly-efficient metal-free organic dyes for dye-sensitized solar cells. Chem Commun 2003;24:3036–7.
[30] Horiuchi T, Miura H, Uchida S. J Photochem Photobiol A 2004;164(1–3): 29–32.
[31] Liu YL, Di CA, Xin YR, Yu G, Liu YQ, He QG, et al. Organic light-emitting diode based on a carbazole compound. Synth Met 2006;156:824–7.
[32] Cervini R, Li XC, Spencer GWC, Holmes AB, Moratti SC, Friend RH. Electrochemical and optical studies of PPV derivatives and poly(aromatic oxadiazoles). Synth Met 1997;84:359–60.
[33] Frisch MJ, Trucks GW, Schlegel HB, Scuseria GE, Robb MA, Cheeseman JR, et al. Gaussian 03, revision D.01. Wallingford, CT: Gaussian, Inc.; 2004.
[34] Becke AD. Density-functional thermochemistry.III. The role of exact exchange. J Chem Phys 1993;98:5648–52.
[35] Ditchfield R, Hehre WJ, Pople JA. Self-consistent molecular-orbital methods. IX. An extended gaussian-type basis for molecular-orbital studies of organic molecules. J Chem Phys 1971;54:724–8.
[36] Dreuw A, Head-Gordon M. Failure of time-dependent density functional theory for long-range charge-transfer excited states: the zincbacteriochlorin-bacterlochlorin and bacteriochlorophyll-spheroidene complexes. J Am Chem Soc 2004;126:4007–16.
[37] Tang CW, VanSlyke SA, Chen CH. Electroluminescence of doped organic thin-films. J Appl Phys 1989;65:3610–6.
[38] Hamada Y, Kanno H, Tsujioka T, Takahashi H, Usuki T. Red organic light-emitting diodes using an emitting assist dopant. Appl Phys Lett 1999;75:1682–4.